

Multistage Complexation of Fluoride Ions by a Fluorescent Triphenylamine Bearing Three Dimesitylboryl Groups: Controlling Intramolecular Charge Transfer

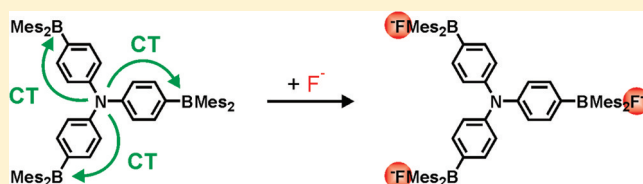
Hauke C. Schmidt,[†] Luisa G. Reuter,[†] Josef Hamacek,[‡] and Oliver S. Wenger^{*,†}

[†]Institut für Anorganische Chemie, Georg-August-Universität Göttingen, Tammannstrasse 4, D-37077 Göttingen, Germany

[‡]Département de Chimie Minérale, Analytique et Appliquée, Université de Genève, 30 quai Ernest-Ansermet, CH-1211 Genève 4, Switzerland

Supporting Information

ABSTRACT: A propeller-shaped boron–nitrogen compound (NB_3) with three binding sites for fluoride anions was synthesized and investigated by optical absorption, luminescence, and (^1H , ^{11}B , ^{13}C , ^{19}F) NMR spectroscopy. Binding of fluoride in dichloromethane solution occurs in three clearly identifiable steps and leads to stepwise blocking of the three initially present nitrogen-to-boron charge transfer pathways. As a consequence, the initially bright blue charge transfer emission is red-shifted and decreases in intensity, until it is quenched completely in presence of large fluoride excess. Fluoride binding constants were determined from global fits to optical absorption and luminescence titration data and were found to be $K_{a1} = 4 \times 10^7 \text{ M}^{-1}$, $K_{a2} = 2.5 \times 10^6 \text{ M}^{-1}$, and $K_{a3} = 3.2 \times 10^4 \text{ M}^{-1}$ in room temperature dichloromethane solution. Complexation of fluoride to a given dimesitylboryl site increases the electron density at the central nitrogen atom of NB_3 , and this leads to red shifts of the remaining nitrogen-to-boron charge transfer transitions involving yet unfluorinated dimesitylboryl groups.

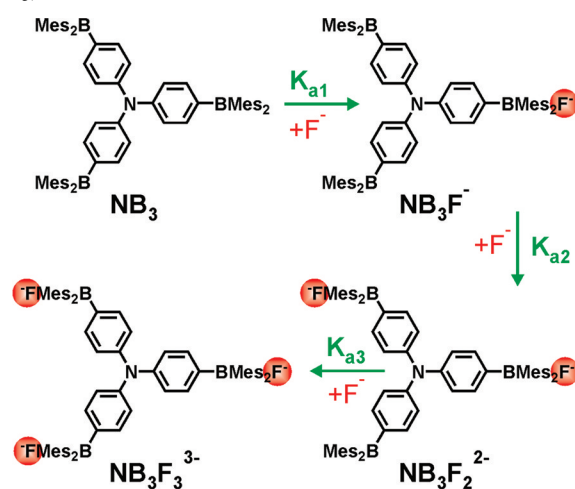


INTRODUCTION

The use of Lewis acidic organoboron compounds for selective binding of fluoride and cyanide anions has received much attention in the past decade.¹ Current challenges in this field include the construction of systems capable of efficient fluoride or cyanide binding from aqueous solution,² the detection of fluoride ions using redox-based sensors,³ fluoride-sensing through tuning of the phosphorescence emitted by metal complexes with triarylborane-substituted ligands,⁴ and the development of new optoelectronic materials.⁵ Much effort is devoted to optimizing the fluoride binding constants, for example, by exploring cationic or bidentate organoboron compounds.⁶ Recently, π -conjugated boron–nitrogen systems have attracted attention because they exhibit intramolecular charge transfer from the electron-rich nitrogen to the electron-poor boron atom, and fluoride complexation strongly alters the electronic properties of these substances.⁷ In the field of organic mixed valence there are several examples of star- or propeller-shaped molecules which exhibit unusual charge delocalization phenomena,⁸ but intramolecular charge transfer in structurally analogous boron–nitrogen systems has so far not been explored.

In this paper we report on the propeller-shaped boron–nitrogen compound tris(4-(dimesitylboryl)phenyl)amine (Scheme 1, upper left corner), hereafter referred to as NB_3 . With three dimesitylboryl groups present in this molecule, the formation of adducts with one (NB_3F^-), two ($\text{NB}_3\text{F}_2^{2-}$), and three fluoride anions ($\text{NB}_3\text{F}_3^{3-}$) may be expected (Scheme 1).

Scheme 1. Tris(4-(dimesitylboryl)phenyl)amine Molecule (NB_3) and Its Fluoride Adducts



The purpose of our research was not to develop a particularly potent fluoride sensor; rather, our work was motivated by a fundamental interest in electron transfer.⁹ Specifically, we sought to explore how stepwise fluoride addition to tris(4-(dimesitylboryl)phenyl)amine affects the three nitrogen-to-boron charge transfer pathways which are initially present in

Received: September 16, 2011

Published: October 13, 2011

this molecule. Such information may be useful for future studies of long-range charge transfer across dimesitylboryl-substituted bridges. There have been several prior investigations of propeller-shaped boryl systems,^{7e,g,h,10} but to the best of our knowledge our study is the first one in which there are three nitrogen-to-boron charge transfer pathways that can be controlled by stepwise fluoride addition.^{7h}

RESULTS AND DISCUSSION

Synthesis. Tris(4-(dimesitylboryl)phenyl)amine (NB₃) can be synthesized in two steps: Bromination of commercially available triphenylamine gives tris(4-bromophenyl)amine, which can be converted to NB₃ through addition of *n*-butyllithium solution, followed by addition of dimesitylboryl fluoride in diethyl ether at -78 °C. The overall yield for the bromination/borylation reaction sequence was 23%, but given our primary interest in the (photo)physical and fluoride binding properties of the target molecule, no particular attempts to optimize reaction yields were undertaken. Detailed synthetic protocols and product characterization data are given in the Experimental Section.

Optical Absorption and Luminescence Titrations. The solid black trace in Figure 1a is the optical absorption spectrum

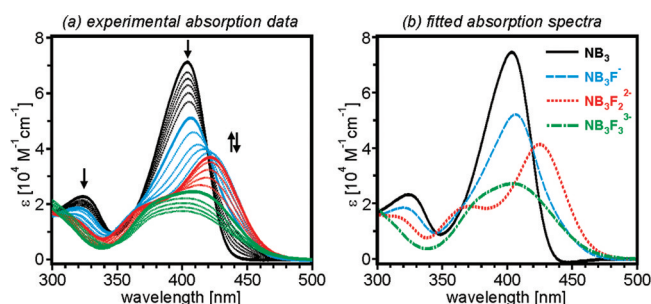


Figure 1. (a) Optical absorption spectra measured on a 1.6×10^{-5} M solution of NB₃ in dichloromethane after addition of increasing amounts of tetrabutylammonium fluoride. The solid black trace is the initial spectrum; the trend of the absorbance at three selected wavelengths is marked by downward or upward arrows. (b) Experimental absorption spectrum of NB₃ (black trace) and fitted absorption spectra of the three fluoride adducts (colored traces) as determined using the SPECIFIT software.¹¹

of a 1.6×10^{-5} M solution of NB₃ in dichloromethane. When adding tetrabutylammonium fluoride (TBAF), the absorbance at 400 nm gradually decreases while at longer wavelengths more complicated behavior is observed. This is illustrated by Figure 2a which shows the titration curve obtained when monitoring the absorbance at 435 nm (open circles). An initial steep increase between 0 and 2 equiv is followed by a more shallow decrease up to 10 equiv, and finally there is an even weaker drop-off above 10 equiv.

Global fits to the experimental absorption data from Figure 1a using the SPECIFIT program¹¹ lead to the conclusion that, starting from the initially present NB₃ species, fluoride addition leads the formation of 1:1, 1:2, and 1:3 adducts between NB₃ and F⁻, as illustrated by Scheme 1.

All other binding models (e.g., a model permitting only the formation of 1:1 and 1:2 adducts) gave either completely unsatisfactory fits or unreasonably high binding constants, or both. The final fit relies on the experimental absorption spectrum of NB₃ (black trace in Figure 1b) and the calculated

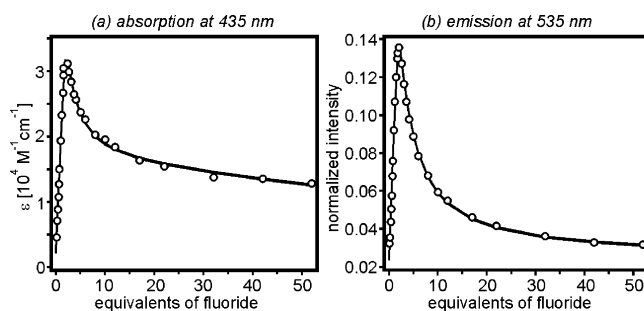


Figure 2. (a) Extinction at 435 nm as a function of fluoride equivalents added to a 1.6×10^{-5} M solution of NB₃ in dichloromethane. (b) Luminescence intensity at 535 nm measured after excitation of the same solution at 363 nm.

adduct absorption spectra represented by the colored traces in Figure 1b. The experimental data in Figure 1a were colored accordingly in order to visualize which one of the four possible species dominates the overall absorption spectrum at a given titration point. As mentioned above, this is a global fit over all wavelengths from 300 to 500 nm, and for a wavelength of 435 nm the quality of the fit is illustrated by the solid line in the titration curve of Figure 2a. Key outcomes of the fit are the titration constants for the individual fluoride anions as summarized in the first row (“abs”) of Table 1. The $\beta_{1,n}$

Table 1. Logarithms of the Cumulative Fluoride Binding Constants Determined from Absorption (“abs”) and Emission (“em”) Data^a

	$\log(\beta_{1,1})$	$\log(\beta_{1,2})$	$\log(\beta_{1,3})$
abs	7.5(5)	13.9(5)	18.4(5)
em	7.7(5)	14.1(5)	18.5(5)
avg	7.6(5)	14.0(5)	18.5(5)

^aThe bottom row (“avg”) contains the average values.

values reported therein are cumulative binding constants for the 1:1 ($\beta_{1,1}$), 1:2 ($\beta_{1,2}$), and 1:3 ($\beta_{1,3}$) adducts, and the error estimate on the last digit is captured by the number given in parentheses.

Before discussing the magnitudes of these binding constants, we note that fluoride addition to a dichloromethane solution of NB₃ does also lead to substantial changes of the emission properties of this solution. As seen from Figure 3a, the luminescence intensity decreases considerably, and there is redistribution of intensity from shorter to longer wavelengths. Excitation occurred at 363 nm, i.e., at a wavelength at which the absorbance is largely constant over the fluoride concentration range relevant here, and hence the decrease in emission intensity observed in Figure 3a reflects a genuine decrease of the overall luminescence quantum yield. Detection at a wavelength of 535 nm yields an emission titration curve (Figure 2b) which is qualitatively similar to the absorption titration curve obtained when detecting at 435 nm (Figure 2a). Again, careful analysis of the experimental data with the SPECIFIT software leads to the inescapable conclusion that 1:1, 1:2, and 1:3 adducts are formed between NB₃ and F⁻. A global fit at all wavelengths between 400 and 700 nm gives the calculated spectra represented by the colored traces in Figure 3b and the cumulative binding constants given in the second row (“em”) of Table 1.

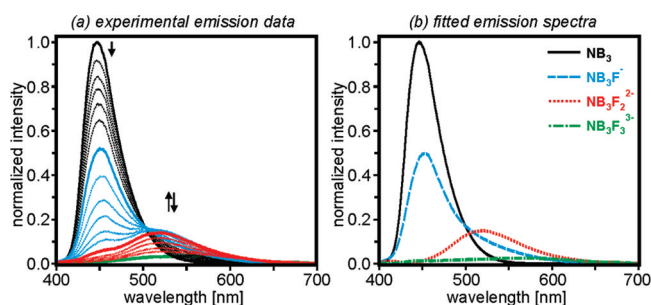


Figure 3. (a) Luminescence spectra measured after 363 nm excitation of a 1.6×10^{-5} M solution of NB_3 in dichloromethane after addition of increasing amounts of tetrabutylammonium fluoride. The solid black trace is the initial spectrum; the trend of the emission intensity at two selected wavelengths is marked by downward or upward arrows. (b) Experimental emission spectrum of NB_3 (black trace) and fitted emission spectra of the three fluoride adducts (colored traces).

The agreement between binding constants determined from absorption and emission data is excellent, and average values are given in the third row (“avg”) of Table 1. The association constants for the individual fluoride binding steps (as defined in Scheme 1) are $K_{a1} = 4 \times 10^7 \text{ M}^{-1}$, $K_{a2} = 2.5 \times 10^6 \text{ M}^{-1}$, and $K_{a3} = 3.2 \times 10^4 \text{ M}^{-1}$. Thus, successive binding of fluoride anions occurs with negative cooperativity: As expected, the buildup of negative charge upon binding of the first fluoride hinders the second fluoride binding step ($\log K_{a2} - \log K_{a1} = 1.2$) and even more the third ($\log K_{a3} - \log K_{a2} = 1.9$). However, compared to other systems with multiple sites for fluoride binding, the extent of negative cooperativity in NB_3 is relatively modest.¹ This is likely due to the fact that the three boron centers are relatively far apart from each other, resulting in comparatively weak electronic communication between individual dimesitylboryl groups.

The observation of a weak yellow emission for $\text{NB}_3\text{F}_3^{3-}$ ($\lambda_{\text{max}} \approx 550 \text{ nm}$ in Figure 3) is somewhat puzzling. Charge transfer emission cannot occur in this species, and $\pi-\pi^*$ emissions would be expected to show up at significantly shorter wavelengths. It appears plausible that the weak yellow emission is due to traces of impurities or degradation products. The apparent intensities of the blue emission from NB_3 and the yellow impurity luminescence are essentially equal (Figure 4a),

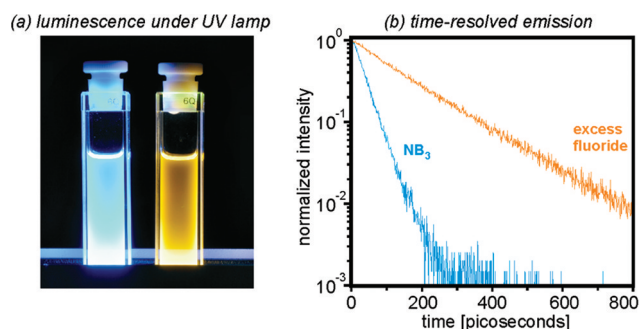


Figure 4. (a) Luminescence of pure NB_3 (left) and of NB_3 in the presence of very large excess (>100 equiv) of fluoride (right). (b) Decays of the luminescences from (a) after pulsed excitation at 340 nm.

but this is only because the two emissions occur in spectral ranges in which the human eye has very different sensitivities. Figure 4b shows the luminescence decays of the blue and

yellow emissions from Figure 4a in dichloromethane after pulsed excitation at 340 nm. The blue charge transfer emission exhibits a lifetime (τ) of 36 ns under these conditions, while the yellow impurity luminescence decays with $\tau = 152 \text{ ns}$. The factor of 4 decrease of the excited-state decay rate constant combined with the factor of 20 decrease in emission quantum yield (estimated from Figure 3a) leads to the conclusion that the two emissions are of fundamentally different origin. This finding is in line with our assignment of the yellow luminescence to an impurity emission.

^{19}F and ^{11}B NMR Spectroscopic Investigations. While optical absorption and luminescence spectroscopy appear as the most sensitive techniques for investigation of fluoride binding to NB_3 (particularly in view the magnitudes of the binding constants), ^{11}B and ^{19}F NMR spectroscopies can provide complementary information regarding fluoride complexation. The result of a ^{19}F NMR titration of NB_3 with tetrabutylammonium fluoride in dichloromethane solution is shown in Figure 5. The sharp signal at -129 ppm , which is easily

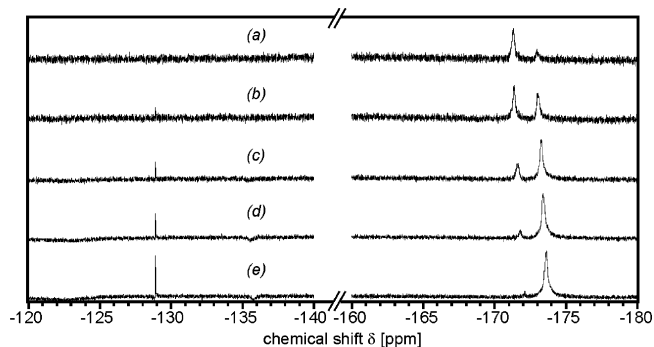


Figure 5. ^{19}F NMR spectra of NB_3 in CD_2Cl_2 in presence of (a) 1, (b) 2, (c) 4, (d) 6, and (e) 10 equiv of tetrabutylammonium fluoride.

noticeable in all spectra except the first one, is caused by the tetrabutylammonium fluoride titrant; i.e., the respective signal is due to unbound fluoride anions. Upon addition of increasing amounts of fluoride, first a resonance at -172 ppm appears and then a second signal at -174 ppm becomes observable. Only the latter signal persists when more than 10 equiv of fluoride is added, but additional resonances are not observed, not even in presence of very large excess (>100 equiv) of fluoride. The -172 and -174 ppm resonances fall into the typical range for dimesitylboryl-bound fluoride;¹ hence, they are attributed to $\text{NB}_3\text{F}_n^{n-}$ ($n = 1-3$) species. Intuitively, one might have expected three individual resonances signaling the presence of 1:1, 1:2, and 1:3 adducts. The ^{19}F NMR titration data in Figure 5 are seemingly in contradiction with this expectation; however, we note that the relative intensities of the -172 and -174 ppm resonances as a function of fluoride concentration are consistent with the species distribution curves obtained from the UV-vis and luminescence titration data (Figure 6) if one assumes that the resonances of $\text{NB}_3\text{F}_2^{2-}$ and $\text{NB}_3\text{F}_3^{3-}$ are superimposed in the signal at -174 ppm . The species distribution curve in Figure 6 predicts that after addition of 1 equiv of fluoride the NB_3F^- species is dominant, while after addition of ~ 2 equiv similar amounts of NB_3F^- and $\text{NB}_3\text{F}_2^{2-}$ will be present. The ^{19}F NMR data in Figure 5a,b are in good agreement with this prediction. After addition of more than 5 equiv of fluoride, the 1:1 adduct is clearly a minority species;

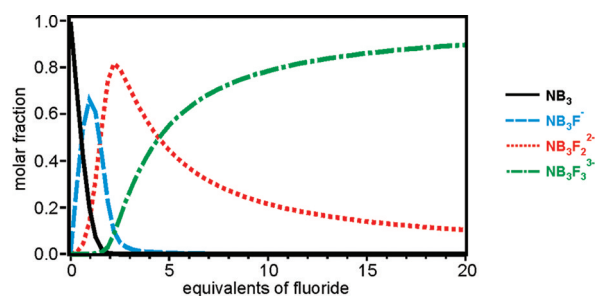


Figure 6. Distribution of individual species as a function of fluoride equivalents added.

hence, the -172 ppm resonance becomes weak (Figure 5d) or even undetectable (Figure 5e).

^{11}B NMR spectroscopy provides additional evidence for binding of fluoride to NB_3 , but the sensitivity of our NMR spectrometer to the ^{11}B nucleus is comparatively low, and hence only qualitative conclusions can be drawn from this data. The ^{11}B NMR spectrum of the initial NB_3 species exhibits a broad resonance at 74 ppm which is typical for dimesitylboryl groups (page S4 in Supporting Information). Addition of 1 equiv of fluoride produces a broad signal around 7 ppm that can be attributed to a fluorinated dimesitylboryl group, in agreement with previously reported chemical shifts for comparable systems.¹ Even when adding 10 equiv of fluoride no additional ^{11}B resonances appear, and thus it is impossible to distinguish between 1:1, 1:2, and 1:3 adducts from this experiment. The comparatively large width of the ^{11}B resonances combined with the low instrument sensitivity is not helpful in this respect.

Charge Transfer Properties. The UV–vis spectrum of NB_3 is dominated by an absorption band at 400 nm (solid black trace in Figure 2a) which is expected to be caused by charge transfer from the electron-rich nitrogen center to the electron-poor dimesitylboryl groups, as commonly the case for conjugated nitrogen–boron compounds.^{7c–g} Upon fluoride addition, one usually observes a blue shift of these charge transfer transitions because the boron-localized LUMO is shifted to higher energy. However, as seen from Figure 2, opposite behavior is observed in the case of the NB_3 molecule: The NB_3F^- spectrum (and even more so the $\text{NB}_3\text{F}_2^{2-}$ spectrum) is significantly red-shifted with respect to the NB_3 spectrum. The likely explanation for this uncommon behavior is that there are multiple charge transfer pathways in our propeller-shaped molecule: Binding of the first fluoride anion blocks only one out of three nitrogen-to-boron charge transfer pathways; moreover, it may even lead to an increase of the electron density at the nitrogen center. Similarly, binding of the second fluoride anion still leaves one nitrogen-to-boron charge transfer pathway open, and the nitrogen center in this case is even more electron-rich. This may explain both the decrease in extinction as well as the red shift of the lowest energetic absorption band along the series NB_3 , NB_3F^- , $\text{NB}_3\text{F}_2^{2-}$. In the case of $\text{NB}_3\text{F}_3^{3-}$ all charge transfer pathways are blocked.

SUMMARY AND CONCLUSIONS

Binding of up to three fluoride anions to NB_3 occurs with comparatively small negative cooperativity and can easily be followed by optical absorption and luminescence spectroscopy, where it manifests itself by spectral changes that can be interpreted by blocking of individual nitrogen-to-boron charge

transfer pathways. Thus, there is control over intramolecular charge transfer along each of the three branches of the propeller-shaped molecule.

On the one hand, the small negative binding cooperativity suggests that the electronic interaction between individual dimesitylboryl groups is small. On the other hand, complexation of fluoride at a given dimesitylboryl site appears to affect the electron density at the central nitrogen atom of NB_3 to a non-negligible extent, leading to a red shift of the remaining (unblocked) nitrogen-to-boron charge transfer transitions. This behavior suggests that when using dimesitylboryl-substituted bridging elements, long-range charge transfer processes in donor–bridge–acceptor molecules could be controlled by fluoride addition.

EXPERIMENTAL SECTION

Synthesis. Bromine (0.62 g, 3.9 mmol) was added dropwise to a stirred solution of triphenylamine (0.40 g, 1.6 mmol) in chloroform (3 mL) at 0 °C. The reaction mixture was stirred for 1 h at 0 °C and for 30 min at room temperature. After filtration through a glass frit, ethanol (10 mL) was added, and the resulting solid was filtered and washed with ethanol. Drying in vacuum gave 0.38 g of tris(4-bromophenyl)amine as a colorless solid (38% yield). ^1H NMR (300 MHz, CDCl_3): δ (ppm) = 6.96–6.93 (m, 6 H), 7.35–7.39 (m, 6 H).

Tris(4-bromophenyl)amine (0.30 g, 0.6 mmol) was dissolved in dry diethyl ether (3 mL) and cooled to -78 °C under a nitrogen atmosphere. While stirring at -78 °C, 1.6 M *n*-butyllithium solution in hexane (1.25 mL, 2.0 mmol) was added dropwise to the tris(4-bromophenyl)amine solution. Subsequently, the reaction mixture was allowed to warm to room temperature, and it was stirred for 1 h at this temperature before it was cooled again to -78 °C. Then, a solution of dimesitylboron fluoride (0.50 g, 1.87 mmol) in dry diethyl ether was added dropwise to the reaction mixture. The latter was allowed to warm to room temperature overnight, and finally 1 M hydrochloric acid (10 mL) was added. After phase separation the aqueous phase was extracted 3 times with 20 mL portions of dichloromethane, and the combined organic phases were dried over anhydrous magnesium sulfate. Solvent evaporation on a rotary evaporator was followed by washing the solid residue with acetone. Drying in vacuum afforded 0.36 g of tris(4-(dimesitylboryl)phenyl)amine (NB_3) as a pale yellow solid (60% yield). ^1H NMR (300 MHz, CDCl_3): δ (ppm) = 2.05 (s, 36 H), 2.31 (s, 18 H), 6.82 (s, 12 H), 7.07 (d, J = 9.7 Hz, 6 H), 7.42 (d, J = 9.7 Hz, 6 H). ^{13}C NMR (300 MHz, CDCl_3): δ (ppm) = 21.2, 23.4, 123.4, 128.1, 138.2, 138.4, 140.7, 149.8. MS (EI): m/z = 989.6 (calcd: 989.87). Anal. Calcd for $\text{C}_{72}\text{H}_{78}\text{NB}_3 \cdot 1.5\text{H}_2\text{O}$ (%): C: 84.97, H: 7.97, N: 1.38. Found: C: 84.71, H: 7.71, N: 1.30.

Spectral Fit Procedures. Statistical treatment of the spectrophotometric titrations in absorption or emission modes was performed with the SPECFIT program.¹¹ The stability constant for the NB_3F^- species was refined after fixing the initially fitted constants for $\text{NB}_3\text{F}_2^{2-}$ and $\text{NB}_3\text{F}_3^{3-}$ because of smooth spectral variations at the beginning of titrations.

ASSOCIATED CONTENT

Supporting Information

^1H , ^{13}C , and ^{11}B NMR data. This material is available free of charge via the Internet at <http://pubs.acs.org>.

AUTHOR INFORMATION

Corresponding Author

*E-mail: oliver.wenger@chemie.uni-goettingen.de.

ACKNOWLEDGMENTS

Inke Siewert is thanked for valuable advice and discussions.

REFERENCES

- (1) Wade, C. R.; Broomsgrove, A. E. J.; Aldridge, S.; Gabbai, F. P. *Chem. Rev.* **2010**, *110*, 3958–3984.
- (2) (a) Kim, Y.; Huh, H. S.; Lee, M. H.; Lenov, I. L.; Zhao, H. Y.; Gabbai, F. P. *Chem.—Eur. J.* **2011**, *17*, 2057–2062. (b) Kim, Y.; Gabbai, F. P. *J. Am. Chem. Soc.* **2009**, *131*, 3363–3369. (c) Lee, M. H.; Agou, T.; Kobayashi, J.; Kawashima, T.; Gabbai, F. P. *Chem. Commun.* **2007**, 1133–1135. (d) Hudnall, T. W.; Gabbai, F. P. *J. Am. Chem. Soc.* **2007**, *129*, 11978–11986. (e) Wade, C. R.; Gabbai, F. P. *Dalton Trans.* **2009**, 9169–9175.
- (3) (a) Aldridge, S.; Bresner, C.; Fallis, I. A.; Coles, S. J.; Hursthouse, M. B. *Chem. Commun.* **2002**, 740–741. (b) Bresner, C.; Day, J. K.; Coombs, N. D.; Fallis, I. A.; Aldridge, S.; Coles, S. J.; Hursthouse, M. B. *Dalton Trans.* **2006**, 3660–3667. (c) Broomsgrove, A. E. J.; Addy, D. A.; Bresner, C.; Fallis, I. A.; Thompson, A. L.; Aldridge, S. *Chem.—Eur. J.* **2008**, *14*, 7525–7529. (d) Dusemund, C.; Sandanayake, K.; Shinkai, S. *J. Chem. Soc., Chem. Commun.* **1995**, 333–334. (e) Li, J.; Zhang, G. X.; Zhang, D. Q.; Zheng, R. H.; Shi, Q. A.; Zhu, D. B. *J. Org. Chem.* **2010**, *75*, 5330–5333.
- (4) (a) Sun, Y.; Hudson, Z. M.; Rao, Y. L.; Wang, S. N. *Inorg. Chem.* **2011**, *50*, 3373–3378. (b) Zhao, S. B.; McCormick, T.; Wang, S. *Inorg. Chem.* **2007**, *46*, 10965–10967. (c) Sun, Y.; Wang, S. N. *Inorg. Chem.* **2009**, *48*, 3755–3767. (d) Lam, S. T.; Zhu, N. A. Y.; Yam, V. W.-W. *Inorg. Chem.* **2009**, *48*, 9664–9670. (e) Zhao, Q.; Li, F. Y.; Liu, S. J.; Yu, M. X.; Liu, Z. Q.; Yi, T.; Huang, C. H. *Inorg. Chem.* **2008**, *47*, 9256–9264. (f) You, Y. M.; Park, S. Y. *Adv. Mater.* **2008**, *20*, 3820–3826. (g) Sakuda, E.; Funahashi, A.; Kitamura, N. *Inorg. Chem.* **2006**, *45*, 10670–10677. (h) Wade, C. R.; Gabbai, F. P. *Inorg. Chem.* **2010**, *49*, 714–720.
- (5) (a) Entwistle, C. D.; Marder, T. B. *Angew. Chem., Int. Ed.* **2002**, *41*, 2927–2931. (b) Elbing, M.; Bazan, G. C. *Angew. Chem., Int. Ed.* **2008**, *47*, 834–838. (c) Yamaguchi, S.; Wakamiya, A. *Pure Appl. Chem.* **2006**, *78*, 1413–1424. (d) Zhao, C. H.; Wakamiya, A.; Inukai, Y.; Yamaguchi, S. *J. Am. Chem. Soc.* **2006**, *128*, 15934–15935. (e) Sundararaman, A.; Venkatasubbiah, K.; Victor, M.; Zakharov, L. N.; Rheingold, A. L.; Jäkle, F. *J. Am. Chem. Soc.* **2006**, *128*, 16554–16565. (f) Li, H. Y.; Sundararaman, A.; Venkatasubbiah, K.; Jäkle, F. *J. Am. Chem. Soc.* **2007**, *129*, 5792–5793. (g) Kinoshita, M.; Kita, H.; Shirota, Y. *Adv. Funct. Mater.* **2002**, *12*, 780–786. (h) Noda, T.; Shirota, Y. *J. Am. Chem. Soc.* **1998**, *120*, 9714–9715. (i) Parab, K.; Venkatasubbiah, K.; Jäkle, F. *J. Am. Chem. Soc.* **2006**, *128*, 12879–12885.
- (6) (a) Hudnall, T. W.; Chiu, C. W.; Gabbai, F. P. *Acc. Chem. Res.* **2009**, *42*, 388–397. (b) Hudnall, T. W.; Kim, Y. M.; Bebbington, M. W. P.; Bourissou, D.; Gabbai, F. P. *J. Am. Chem. Soc.* **2008**, *130*, 10890–10891. (c) Solé, S.; Gabbai, F. P. *Chem. Commun.* **2004**, 1284–1285. (d) Chiu, C. W.; Kim, Y.; Gabbai, F. P. *J. Am. Chem. Soc.* **2009**, *131*, 60–61. (e) Sun, Y.; Ross, N.; Zhao, S. B.; Huszarik, K.; Jia, W. L.; Wang, R. Y.; Macartney, D.; Wang, S. N. *J. Am. Chem. Soc.* **2007**, *129*, 7510–7511.
- (7) (a) Entwistle, C. D.; Marder, T. B. *Chem. Mater.* **2004**, *16*, 4574–4585. (b) Liu, X. Y.; Bai, D. R.; Wang, S. N. *Angew. Chem., Int. Ed.* **2006**, *45*, 5475–5478. (c) Hudson, Z. M.; Liu, X. Y.; Wang, S. N. *Org. Lett.* **2011**, *13*, 300–303. (d) Zhou, G.; Baumgarten, M.; Müllen, K. *J. Am. Chem. Soc.* **2008**, *130*, 12477–12484. (e) Pron, A.; Zhou, G.; Norouzi-Arasi, H.; Baumgarten, M.; Müllen, K. *Org. Lett.* **2009**, *11*, 3550–3553. (f) Liu, Z. Q.; Shi, M.; Li, F. Y.; Fang, Q.; Chen, Z. H.; Yi, T.; Huang, C. H. *Org. Lett.* **2005**, *7*, 5481–5484. (g) Yuan, M. S.; Liu, Z. Q.; Fang, Q. *J. Org. Chem.* **2007**, *72*, 7915–7922. (h) Stahl, R.; Lambert, C.; Kaiser, C.; Wortmann, R.; Jakober, R. *Chem.—Eur. J.* **2006**, *12*, 2358–2370.
- (8) (a) Hankache, J.; Wenger, O. S. *Chem. Rev.* **2011**, *111*, 5138–5178. (b) Bonvoisin, J.; Launay, J. P.; Van der Auweraer, M.; De Schryver, F. C. *J. Phys. Chem.* **1994**, *98*, 5052–5057. (c) Sedó, J.; Ruiz, D.; VidalGancedo, J.; Rovira, C.; Bonvoisin, J.; Launay, J.-P.; Veciana, J. *Adv. Mater.* **1996**, *8*, 748–752. (d) Lambert, C.; Nöll, G. *Angew. Chem., Int. Ed.* **1998**, *37*, 2107–2110. (e) Sun, D.; Rosokha, S. V.; Kochi, J. K. *Angew. Chem., Int. Ed.* **2005**, *44*, 5133–5136. (f) Hirao, Y.; Ito, A.; Tanaka, K. *J. Phys. Chem. A* **2007**, *111*, 2951–2956.
- (9) (a) Wenger, O. S. *Acc. Chem. Res.* **2011**, *44*, 25–35. (b) Wenger, O. S. *Chem. Soc. Rev.* **2011**, *40*, 3538–3550. (c) Hankache, J.; Wenger, O. S. *Chem. Commun.* **2011**, *47*, 10145–10147. (d) Hanss, D.; Walther, M. E.; Wenger, O. S. *Chem. Commun.* **2010**, *46*, 7034–7036. (e) Hanss, D.; Wenger, O. S. *Inorg. Chem.* **2008**, *47*, 9081–9084. (f) Hanss, D.; Wenger, O. S. *Inorg. Chem.* **2009**, *48*, 671–680. (g) Walther, M. E.; Grilj, J.; Hanss, D.; Vauthey, E.; Wenger, O. S. *Eur. J. Inorg. Chem.* **2010**, 4843–4850. (h) Walther, M. E.; Wenger, O. S. *ChemPhysChem* **2009**, *10*, 1203–1206. (i) Hanss, D.; Walther, M. E.; Wenger, O. S. *Coord. Chem. Rev.* **2010**, *254*, 2584–2592. (j) Hanss, D.; Wenger, O. S. *Eur. J. Inorg. Chem.* **2009**, 3778–3790. (k) He, B.; Wenger, O. S. *J. Am. Chem. Soc.* **2011**, DOI: 10.1021/ja207025x. (l) Walther, M. E.; Wenger, O. S. *Inorg. Chem.* **2011**, DOI: 10.1021/ic201446x. (m) Wenger, O. S. *Chem.—Eur. J.* **2011**, *17*, 11692–11702.
- (10) (a) Yamaguchi, S.; Akiyama, S.; Tamao, K. *J. Am. Chem. Soc.* **2000**, *122*, 6335–6336. (b) Yamaguchi, S.; Akiyama, S.; Tamao, K. *J. Am. Chem. Soc.* **2001**, *123*, 11372–11375.
- (11) Gampp, H.; Maeder, M.; Meyer, C. J.; Zuberbühler, A. D. *Talanta* **1986**, *33*, 943–951.